NeuroImage **14,** 632–641 (2001)
doi:10.1006/nimg.2001.0851, available online at http://www.idealibrary.com on IDEAL®

Asymmetrical Activation of Human Visual Cortex Demonstrated by Functional MRI with Monocular Stimulation

A. T. Toosy,* D. J. Werring,* G. T. Plant,† E. T. Bullmore,‡ D. H. Miller,* and A. J. Thompson*

**NMR Research Unit, Institute of Neurology, and †The National Hospital for Neurology and Neurosurgery, Queen Square, London WC1N 3BG, United Kingdom; and ‡Department of Psychiatry, University of Cambridge, Addenbrooke's Hospital, Cambridge CB2 2QQ, United Kingdom*

Received September 26, 2000; published online July 10, 2001

We have demonstrated asymmetric activation patterns in the visual cortices of normal humans who have undergone functional MRI with monocular photic stimulation. The contralateral hemisphere is activated more strongly and to a greater spatial extent than the ipsilateral hemisphere when either eye is stimulated. This asymmetry can be explained by nasotemporal asymmetries which have been described in anatomical studies of the visual system in primates and humans. In part, the representation of the monocular crescent of the temporal hemifield of either eye, which exists only in the crossed projection, may explain this. In addition, within the binocular field, there is a biased crossed projection of nasal retinal ganglion cells which drive the contralateral ocular dominance columns in V1. Finally, the blind spot representation in the ipsilateral visual cortex may also contribute to the observed asymmetries. Our study may in effect provide a functional correlate of the anatomical asymmetries that have been observed in humans and animals.

INTRODUCTION

It is well known that in most mammals with frontal eyes, each retina projects to both cerebral hemispheres by means of the chiasmal hemidecussation. Ganglion cells in the temporal retina give rise to axons that are uncrossed in the optic chiasm and project to the ipsilateral hemisphere, while axons from nasal ganglion cells are crossed and project to the contralateral hemisphere (Polyak, 1957; Stone and Hansen, 1966). Studies using neuroanatomical tracer or degeneration techniques have confirmed this structural arrangement (Itaya and van Hoesen, 1982; Tootell *et al.,* 1988). Hemidecussation allows retinogeniculate axons conveying information from the right homonymous hemifields to project to ocular dominance columns (ODCs)[1] in the left cerebral hemisphere and vice versa (Hubel and Wiesel, 1968, 1969). This arrangement allows signals from retinal regions corresponding to a particular point in the visual field from both the right and the left eyes to converge to adjacent ODCs, thus facilitating binocular interactions.

The *functional* representation of each retina has until recently been difficult to investigate. However, with the advent of functional neuroimaging techniques, including positron emission tomography and functional magnetic resonance imaging (fMRI), it has become possible to study patterns of cerebral activation in response to controlled visual stimulation of visual field areas and thus to map their representation in the visual cortex.

fMRI can detect regional brain activity by virtue of small changes in blood oxygenation that accompany neural activity (the blood oxygenation level-dependent or BOLD effect). It represents a powerful tool with which to investigate brain function noninvasively and has been increasingly used in studies of the visual system. A number of studies have mapped the cortical representation of the visual field during phase-encoded visual stimulation (Sereno *et al.,* 1995; Tootell *et al.,* 1998). However, such studies have not yet found widespread clinical application. One of the earliest and simplest stimuli to be employed for fMRI is a flashing red LED display mounted in each eyepiece of a pair of light-proof goggles (see, for example, Belliveau *et al.,* 1991; Kwong *et al.,* 1992; Ogawa *et al.,* 1992). Monocular stimulation of this type has been used to study the pattern of cerebral activation induced by stimulating each eye in control subjects or in patients with a variety of neurological disorders (e.g., Hedera *et al.,* 1994; Howard *et al.,* 1995; Miki *et al.,* 1996; Rombouts *et al.,* 1998). Where pathology can be localized

[1] Abbreviations used: PSC, presumed striate cortex; ODC, ocular dominance columns; fMRI, functional magnetic resonance imaging; BOLD, blood oxygenation level-dependent; FPQ, fundamental power quotient; ANOVA, analysis of variance.

1053-8119/01 $35.00

TABLE 1

Activated Volumes in Presumed Striate Cortex from Individual Activation Maps in the 20- and 40-s Epoch Groups of Volunteers

	Left eye stimulation		Right eye stimulation	
	Left PSC activation/cm^3	Right PSC activation/cm^3	Left PSC activation/cm^3	Right PSC activation/cm^3
		20-s epoch group		
	1.94 (21.6%)	7.06 (78.4%)	10.59 (72.4%)	4.03 (27.6%)
	4.43 (27.9%)	11.46 (72.1%)	16.03 (58.3%)	11.48 (41.7%)
	10.21 (42.9%)	13.58 (57.1%)	16.19 (60.8%)	10.43 (39.2%)
	12.04 (41.7%)	16.84 (58.3%)	18.39 (54.1%)	15.61 (45.9%)
	6.94 (48.5%)	7.38 (51.5%)	0.55 (73.3%)	0.2 (26.7%)
	6.14 (37.0%)	10.44 (63.0%)	17.53 (57.2%)	13.11 (42.8%)
	2.24 (26.4%)	6.23 (73.6%)	11.20 (53.7%)	9.66 (46.3%)
Mean (20 s)	6.28 (35.1%)	10.43 (64.9%)	12.93 (61.4%)	9.22 (38.6%)
Paired *t* test	$P = 0.002$ ($P = 0.008$)		$P = 0.005$ ($P = 0.010$)	
		40-s epoch group		
	4.47 (31.6%)	9.68 (68.4%)	0.68 (87.2%)	0.1 (12.8%)
	1.01 (19.8%)	4.08 (80.2%)	11.43 (56.3%)	8.86 (43.7%)
	13.43 (38.6%)	21.35 (61.4%)	3.94 (78.0%)	1.11 (22.0%)
	6.54 (38.5%)	10.44 (61.5%)	11.37 (56.3%)	7.40 (39.4%)
	2.46 (31.7%)	5.31 (68.3%)	5.30 (57.2%)	3.97 (42.8%)
	10.73 (38.9%)	16.87 (61.1%)	9.06 (56.1%)	7.08 (43.9%)
	6.44 (43.3%)	8.44 (56.7%)	9.29 (57.6%)	6.84 (42.4%)
	1.11 (23.9%)	3.53 (76.1%)	5.41 (66.6%)	2.71 (33.4%)
Mean (40 s)	5.77 (33.3%)	9.96 (66.7%)	7.06 (65.0%)	4.76 (35.0%)
Paired *t* test	$P = 0.001$ ($P = 0.001$)		$P < 0.001$ ($P = 0.008$)	
Overall mean	6.01 (34.2%)	10.18 (65.8%)	9.80 (63.3%)	6.84 (36.7%)

Note. The activated volumes on each side of the presumed striate cortex are given as a percentage (in parentheses after each value of activated volume). Paired *t* test results are also shown comparing right versus left PSC activation for left and right eye stimulation conditions in both the 20- and the 40-s epoch groups. *P* values in parentheses show significance of paired *t* tests on the percentages derived from activated volumes for each subject. No statistical comparison for the overall group was performed. PSC, presumed striate cortex.

to the anterior visual pathways (i.e., the retina or optic nerve) investigators have compared activation from affected and unaffected eyes to determine the effects of the pathological process (Miki *et al.*, 1996; Rombouts *et al.*, 1998; Werring *et al.*, 2000). A basic premise in such study designs is that, in the absence of pathology, monocular stimulation of either eye will give a similar anatomical distribution of visual cortex activation. The normal pattern of cerebral activation induced by a simple monocular stimulus is therefore of interest and may be relevant to the interpretation of clinical studies. Although others have reported on the area of visual cortex activated during monocular stimulation (Rombouts *et al.*, 1996), there has been no specific study of the anatomical distribution of the cerebral response to monocular stimulation. We therefore studied normal controls to establish the validity, or otherwise, of the assumption that each eye would induce a similar pattern of cerebral activation in normal subjects.

METHODS

Fifteen normal volunteers (mean age 31.0 years; 7 male, 8 female) were studied. No subjects had any history of neurological illness or any visual symptoms apart from refractive errors. All subjects gave informed written consent. The study was approved by the Joint Ethics Committee of the National Hospital and the Institute of Neurology.

Imaging

Structural MRI. Gradient echo EPI MR images were acquired using a 1.5-T GE Signa Horizon Echospeed system (General Electric, Milwaukee, WI) using a standard quadrature head coil. Multishot, high-resolution mildly T2-weighted EPI near-axial images of the whole brain were obtained (TR = 6000 ms, TE = 40 ms, matrix 256 × 256, FOV 24 cm).

Functional MRI. One-hundred twenty T2*-weighted single-shot EPI images depicting BOLD contrast were

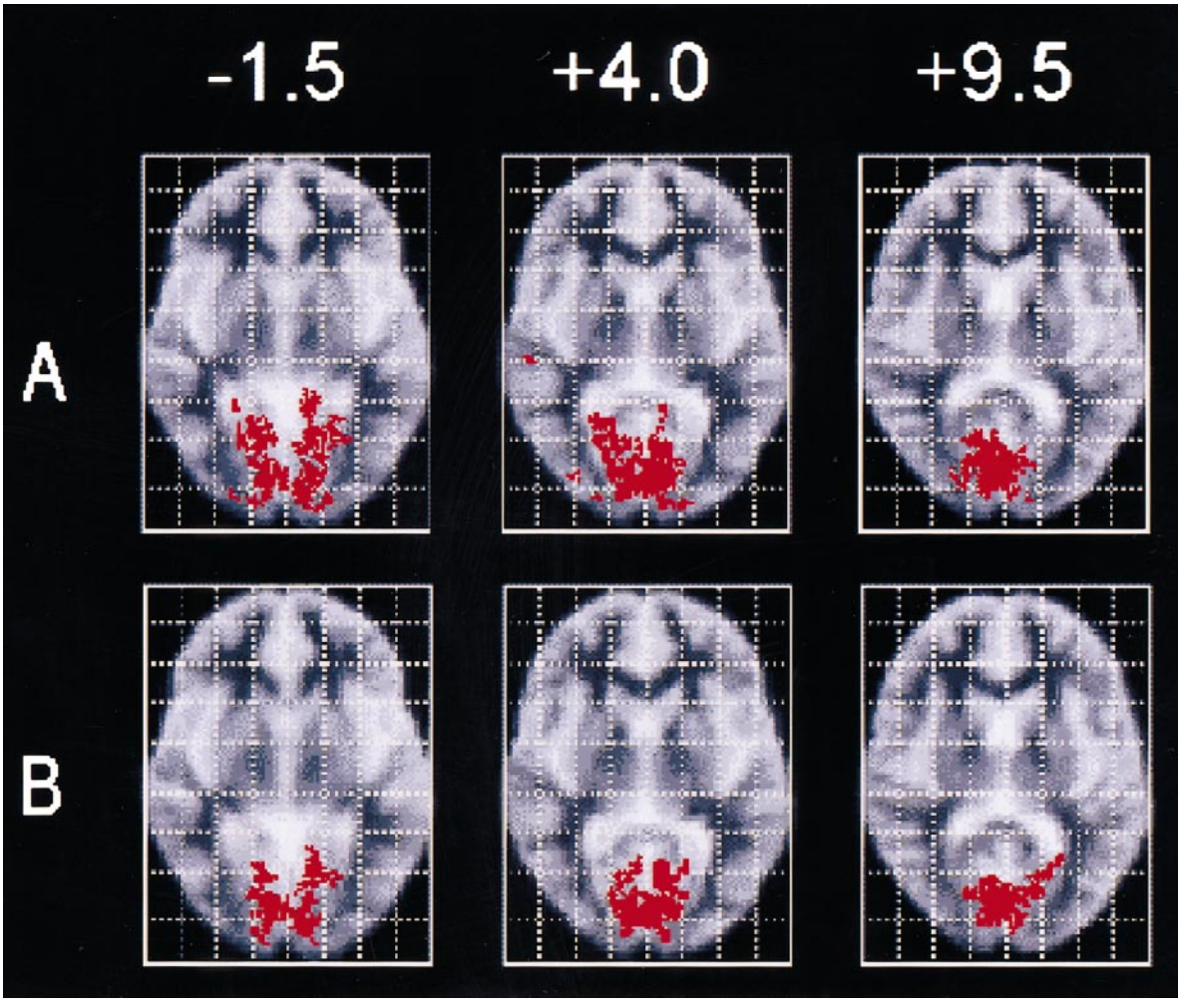

FIG. 1. Generic brain activation maps of normal human controls after stimulation of the left (A) and right (B) eyes with 20-s epochs. Talairach *z* coordinates are indicated above the generic map slices. The right side of the brain is to the left of the figure.

acquired in each 8-min experiment at each of 10 near-axial noncontiguous 5-mm-thick slices through visual cortex approximately parallel to the AC–PC line (TE = 40 ms; TR = 4000 ms; FOV 24 cm; matrix, 96 × 96; in-plane resolution, 2.5 mm; interslice gap, 0.5 mm, flip angle, 90°). Voxel size was therefore 2.5 × 2.5 × 5 mm.

Experimental Design

Subjects passively viewed visual stimuli which alternated periodically between epochs of two contrasting conditions: (A) red 8-Hz photic stimulation to the visual field was presented to one eye using the light-proof goggles while the other eye received no visual stimulation; or (B) no visual stimulation (darkness) was presented to both eyes. The light-proof goggles provided effectively a full-field (Ganzfeldt) photic stimulus. Two groups of subjects were each subjected to two different epoch lengths, one of 20 s and of 40 s, since the cerebral activation detected by the BOLD response has been shown to vary with the frequency of periodic alternation (Thomas and Menon, 1998). The results from the present study should therefore be relevant to the majority of block design studies likely to be performed in clinical studies (most investigators use an epoch length of approximately 30 s). With the 20-s epoch length (used in seven subjects), 12 cycles of alternation between the A and B conditions were presented over the course of each experiment, while with the 40-s epoch length (used in eight subjects), 6 cycles of alternation were presented. Condition B (no stimulation) was always presented first. Each subject was studied once for each side of monocular stimulation; the order of experiments was random.

Analysis

Detailed descriptions of the analysis methods used in this study are provided elsewhere (Brammer *et al.*, 1997; Bullmore *et al.*, 1996), but the essential steps are summarized as follows. Images were corrected for head

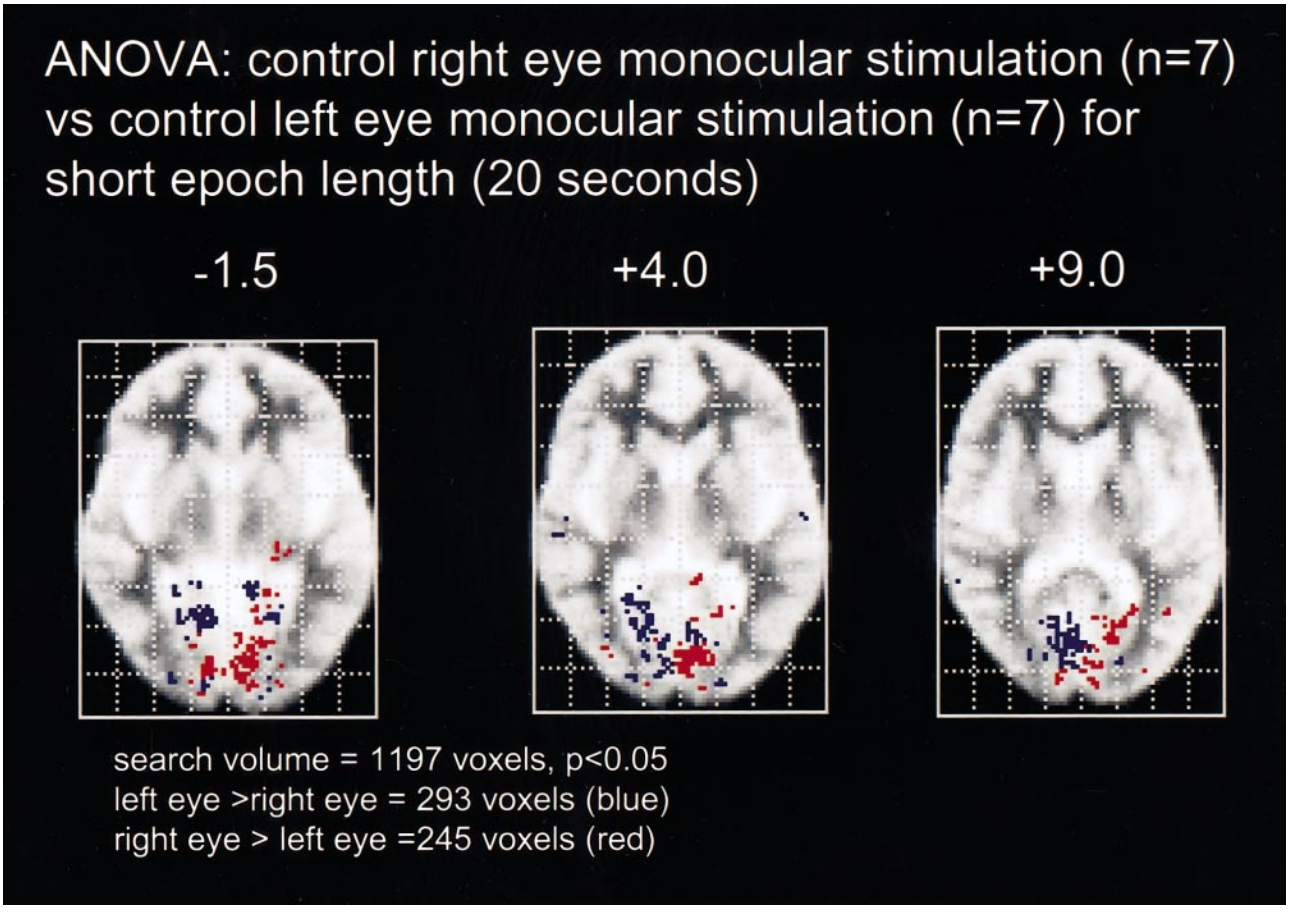

FIG. 2. One-way ANOVA model fitted to generic brain activation maps from monocular stimulation experiments in normal controls with 20-s epochs. Blue voxels are those showing a greater power of response during left eye stimulation; red voxels show a more powerful response during right eye stimulation. Note that left eye stimulation induces stronger activation mainly in right-sided cortex and vice versa. Talairach *z* coordinates are indicated above each generic map slice. The right side of the brain is to the left of the figure.

motion prior to time series analysis (Bullmore *et al.*, 1999). A sinusoidal regression model was fitted by iterated least squares to estimate the power of experimentally determined signal change at the frequency of alternation between A and B conditions while allowing for residual temporal autocorrelation (modeled as a first-order autoregressive process) in the data. The model included sine and cosine waves at the (fundamental) frequency of alternation between A and B conditions to adapt to locally variable hemodynamic delay. The standardized power of response, or fundamental power quotient (FPQ), was defined by the sum of squared amplitudes of the sine and cosine waves divided by their standard errors (Bullmore *et al.*, 1996). Activated voxels were identified in each individual image by a permutation test of FPQ with one-tailed voxelwise probability of type 1 error $P < 0.001$ (Bullmore *et al.*, 1996) and colored red against the gray-scale background of the individual EPI data to form a brain activation map.

Measuring the activated volume. The area of activation in the primary visual cortex (V1) was determined by outlining activated voxels on the brain activation map using a semiautomated contouring technique (DispImage, D. Plummer, UCL, London, UK). The maps were blinded before analysis and all the activated voxels and clusters of voxels adjacent to the calcarine sulcus were selected using *a priori* knowledge of visual neuroanatomy thus targeting the primary visual cortex. The total activated volumes for each subject in right and left primary visual cortices were computed. Since retinotopy was not used to delineate V1, the selected regions and volume measurements that targeted the primary visual cortex will be referred to as "presumed striate cortex" or "PSC" in this article.

Generic brain activation mapping. Maps identifying voxels activated "on average" over all subjects under each experimental condition were constructed in the standard space of Talairach and Tournoux (1988) as described in detail by Brammer *et al.* (1997). This was required for between-experiment comparisons to be performed using an analysis of variance (ANOVA) analysis, which is described in the next section. The rotations, translations, and linear rescaling factors re-

quired to minimize the gray-scale differences between the structural and functional datasets were derived. The same processing steps were used to minimize the gray-scale differences between the histogram-matched, rescaled EPI structural data set and a template in Talairach space created by transforming the high-resolution structural data sets from a group of healthy subjects into standard space using AFNI software (Cox, 1995) and then averaging all of the images. The transformations defining the previous two steps (i.e., structural to functional and structural to Talairach) were sequentially applied to the observed and randomized FPQ maps, and the FPQ values were written to new locations in standard space by nearest-neighbor interpolation. All maps were smoothed by a 2D Gaussian filter with full width at half-maximum = 5 mm to accommodate error in estimation of transformation parameters and individual variability in sulcogyral anatomy. A permutation test of median FPQ at each intracerebral voxel with one-tailed voxelwise probability of type 1 error $P < 0.0001$ was performed. Generically activated voxels were colored red and superimposed on the gray-scale background of the template EPI image in standard space to form a generic brain activation map.

Between-experiment comparisons. The power of periodic response was compared between experiments (left and right monocular stimulation) by fitting a repeated-measures ANOVA model at each intracerebral voxel:

$$FPQ = \mu + \beta \cdot F + \varepsilon,$$

where μ is the overall mean power at a given voxel, F is a factor coding stimulated eye (right or left), and ε is an error. The coefficient β was tested by permutation only at those voxels that were generically activated in one or both of the groups of data being compared (Bullmore *et al.*, 1999). For these analyses, we set the two-tailed voxelwise probability of false-positive error $P = 0.05$. This relatively lenient threshold is justified by the use of a restricted search volume for between-group comparisons, comprising only those voxels that were generically activated in one or both of the experiments analyzed separately. The ANOVA effectively provided a way of comparing the strength of activation in the visual cortex between left and right eye stimulation conditions in both the 20- and 40-s epoch groups.

RESULTS

Twenty-Second Epoch Length

The activated volume results are presented in Table 1. All subjects studied activated visual cortex in response to stimulation of either eye. In all seven cases, left eye stimulation induced a greater volume of right presumed striate cortex activation than left (mean 10.43 vs 6.28 cm^3). In all seven cases, right eye stimulation induced a larger volume of left presumed striate cortex activation than right (mean 12.93 vs 9.22 cm^3). Paired *t*-tests were performed on both groups of left and right eye stimulation, comparing right vs left PSC activation and the results were highly significant (Table 1). The total mean volume of activation was greater with right eye stimulation when compared to left eye stimulation. (22.15 vs 16.71 cm^3) but this was not found to be significant when a paired *t* test was performed on total PSC activation (left PSC + right PSC) comparing left with right eye stimulation ($P = 0.176$). In the generic brain activation maps (Figs. 1A and 1B), activation in response to the stimulation of either eye was demonstrated almost exclusively in visual cortical areas (approximate Brodmann areas 17–19). A visual impression of asymmetry on direct observation of the activation patterns between the left and right eyes (left eye stimulation apparently inducing a larger area of right visual cortex activation, and right eye stimulation inducing a greater area of left visual cortex activation) was noted. Repeated-measures one-way analysis of variance, to compare the strength of activation between sides, showed regions in each hemisphere responding more powerfully to contralateral eye than ipsilateral eye stimulation (Fig. 2).

Forty-Second Epoch Length

Activation was also demonstrated exclusively in visual areas. As in the previous study, monocular stimulation resulted in an asymmetric visual cortex activation pattern, with a larger activated volume in contralateral compared to ipsilateral PSC (for all experiments, Table 1). Paired *t* tests were again performed to compare the left PSC activation volumes with right in both left and right eye stimulation groups ($P \leq 0.001$). Repeated-measures one-way analysis of variance comparing the power of response to right and left eye stimulation showed regions in each hemisphere responding with greater power to contralateral monocular stimulation (Fig. 3). The total mean volume of activation was greater with left eye stimulation when compared to right (15.73 vs 11.82 cm^3) but this was found not to be statistically significant (paired *t* test, $P = 0.446$). The generic brain activation maps again demonstrate a visual impression of asymmetry in the visual cortices (Fig. 4).

DISCUSSION

This study provides new observations on the pattern of cerebral activation in response to monocular visual stimulation in healthy individuals. The results reported have clearly shown an interhemispheric asymmetry in both the power and the anatomical distribu-

tion of the visual cortical response to monocular visual stimulation of each eye in normal controls. The fact that a similar result was obtained in two different control populations studied using two different experimental epoch lengths indicates that the finding is robust. The main findings are, first, a consistent hemispheric asymmetry of visual cortical response, with a larger area activated in the hemisphere contralateral to the stimulated eye (Table 1) and second, the demonstration of areas in each hemisphere in which the power of response was greater during stimulation of the contralateral than the ipsilateral eye (Figs. 2 and 3). These findings are relevant to the interpretation of data obtained in patient fMRI studies using monocular stimulation and are in keeping with existing neuroanatomical and neurophysiological data on visual cortex organization.

It may be noted that with some slices in Figs. 1 and 4 that the activation patterns look strikingly different. It is unclear why this is so. It should be emphasized that the generic brain activation maps were produced to illustrate a visual impression of asymmetry between left and right visual cortex activation. These asymmetries were substantiated with further statistical analysis which took into account measures of and parameters from the whole primary visual cortex. In addition, these figures reveal just a small proportion of the total volume of visual cortex that was sampled. There are little functional data on normal controls who have undergone monocular stimulation and, as far as we are aware, no previous studies have specifically addressed the issue of lateralization of activation. Consequently, data on the expected appearance of such activation maps have not been well established. Nevertheless, further studies may be needed to shed light on this observation.

The asymmetric pattern of cortical activation that we have demonstrated was not noted in previous studies using monocular stimulation (Hedera *et al.*, 1994; Miki *et al.*, 1996; Rombouts *et al.*, 1998). This may be because these earlier studies relied upon the deployment of either one or two slices through the striate cortex for the acquisition of functional data. As a result, it would be difficult to account for visual cortex activation above or below these slices. Our study used 10 slices of 5-mm thickness (with 0.5-mm gaps) through the whole visual cortex and would have encompassed the vertical extent of visual cortex activation (90% coverage with 10% loss due to the interslice gap). In addition, our findings are consistent with several lines of evidence showing an increased anatomical representation of each retina in the contralateral hemisphere. These are discussed below.

First, it is known that in the cortex of the occipital lobe, the most anterior part of the striate cortex harbors projections from a crescentic portion of the contralateral nasal retina which in turn subserves the temporal crescent of the visual field (Horton *et al.*, 1990; Walsh, 1974). This monocular crescent has no ipsilateral projections to the striate cortex; i.e., it fully crosses to the contralateral visual cortex. The greater spatial extent anteriorly of voxel activation that has been observed can be explained at least in part by the representation of the monocular crescent of the visual field.

Second, there is an anatomical asymmetry in retinal ganglion cell density between temporal and nasal retina. The retinal ganglion cell density has been found to be up to two to three times greater in the nasal retina compared to the temporal retina in a primate study (Perry and Cowey, 1985) and 1.2 to 1.8 times greater in the nasal periphery compared to the temporal region at the same eccentricities in owl monkey (Silveira *et al.*, 1993). Thus a bias in favor of nasal retinal ganglion cells could contribute to our findings. This will be valid if the geniculocortical projections to V1 reflect the asymmetry observed at the level of the retinal ganglion cells. In favor of this is the observation that the ratio of crossed to uncrossed fibers at the chiasm is biased toward crossed fibers. Kupfer *et al.* (1967) found a ratio of crossed:uncrossed optic nerve fibers in the optic chiasm of a 78-year-old male to be 53:47. Other studies in humans and primates have found that this asymmetry is further enhanced at the level of the lateral geniculate nucleus, reaching a crossed:uncrossed ratio of approximately 60:40 (Chacko, 1948; Connolly and Van Essen, 1984; Le Gros Clark, 1941). Thus, not only is the greater density of retinal ganglion cells in the nasal retina reflected in the proportion of crossing fibers at the chiasm, there also may be amplification of this distinction at the next synapse.

There is another hypothesis to account for the greater proportion of crossed relative to uncrossed nerve fibers arising from the retina: some temporal axons may cross at the chiasm. This not only has the effect of adding to the fiber load of crossed projections, which will mainly be subserved by nasal retinal ganglion cells, but also subtracts from the uncrossed nerve fiber load. In the cat there is indeed evidence that some fibers arising from the temporal retina project contralaterally (Stone, 1966). However, this anatomical projection pattern has not been confirmed in primates. Studies in primates have demonstrated that there is no overlap between the temporal and nasal projections of retinal ganglion cells except for a narrow vertically oriented median strip (the nasotemporal division), which is about 1° and is centered about the fovea. Within this strip ganglion cells appear to project equally to both contralateral and ipsilateral sides (Stone *et al.*, 1973). Therefore, we believe that since the hypothesis of temporal axon decussation in higher mammals is not substantiated by the available literature, it probably does not contribute to our findings.

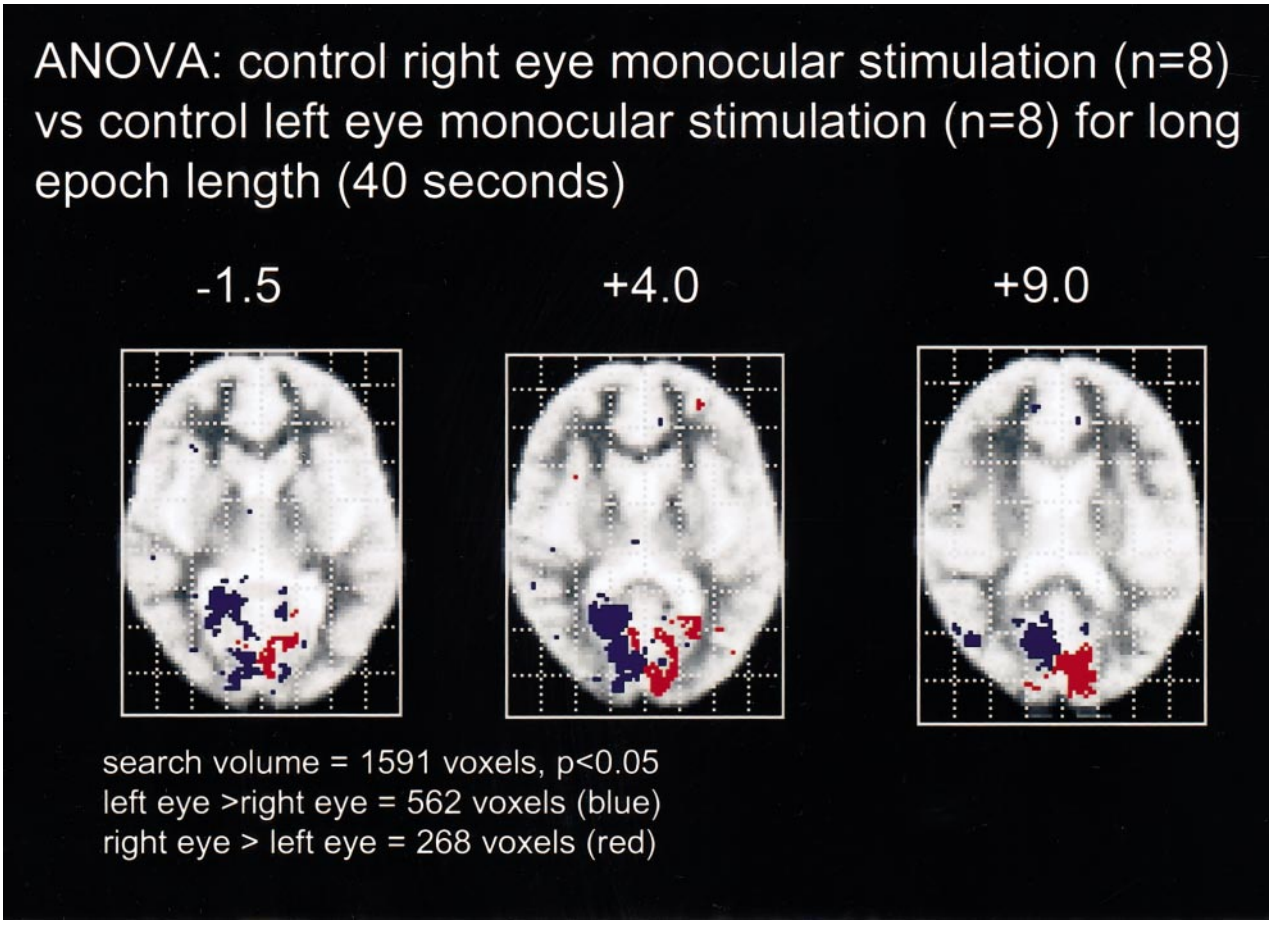

FIG. 3. One-way ANOVA model fitted to generic brain activation maps from monocular stimulation experiments in normal controls with 40-s epochs. Blue voxels are those showing a greater power of response during left eye stimulation; red voxels show a more powerful response during right eye stimulation. Note that left eye stimulation induces stronger activation mainly in right-sided cortex and vice versa. Talairach *z* coordinates are indicated above each generic map slice. The right side of the brain is to the left of the figure.

Studies of visual cortical organization have been found to favor input from the contralateral over the ipsilateral eye. A study published by LeVay *et al.* (1985) examined the ocular dominance columns in the striate cortex of the macaque monkey by autoradiography. ODCs are thin strips of cortex oriented perpendicular to the cortical surface and preferentially receive input from one eye. They constitute the fundamental functional units of the visual cortex (Hubel and Wiesel, 1969). In LeVay *et al.*'s study a profound ocular imbalance between ipsilateral and contralateral eye inputs was found: the ocular dominance stripes in the striate cortex, for the contralateral eye, were found to be significantly wider than those for the ipsilateral eye. These anatomical observations correlate with the functional asymmetry found in our study. LeVay proposed that the imbalance might be a naturally occurring form of visual deprivation due to the partial obstruction of the nasal visual field (which is subserved by the ipsilaterally projecting temporal retina) by the nose. In support of this, the pattern of ocular dominance stripes seen in this study qualitatively matches that seen after experimentally produced monocular deprivation (LeVay *et al.*, 1980). It is not clear how this theory might relate to the differences at the level of the retinal ganglion cell and lateral geniculate nucleus referred to above. Several other studies have documented nasotemporal asymmetries in ODC width or area in primates with a consistent bias favoring inputs from the nasal retina (Rosa *et al.*, 1988; Tychsen and Burkhalter, 1997). Tychsen and Burkhalter found that approximately 55–60% of the ODC area in V1 was subserved by nasal retinal projections in macaque monkeys.

A further possibility may also contribute to our findings. The asymmetries may arise if one eye generates stronger neural activity in V1 binocular cells rather than having a larger number of monocular cells. If this were the case, one would still see lots of activated cortex in the analyses that were conducted. Thus the asymmetry might be one of strength of representation

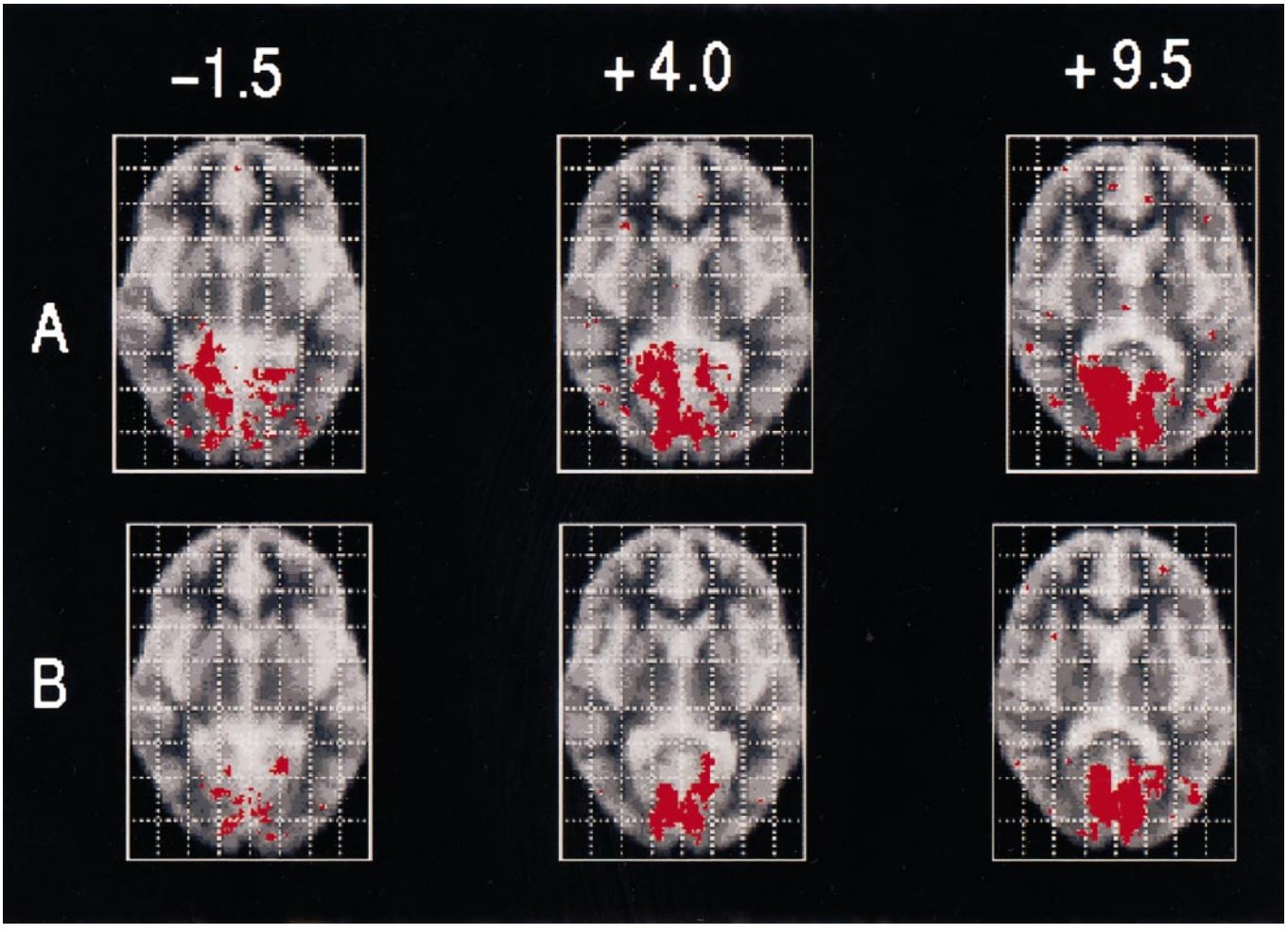

FIG. 4. Generic brain activation maps of normal human controls after stimulation of the left (A) and right (B) eyes with 40-s epochs. Talairach *z* coordinates are indicated above the generic map slices. The right side of the brain is to the left of the figure.

rather than size. This is speculative, although the ANOVA comparisons did demonstrate increased contralateral strength of activation.

An interesting question concerns the representation of the blind spot in V1. It is known that the blind spot is a photoreceptor-free zone and produces mostly monocular, ipsilateral eye representations in V1 and visually can be represented by an "island" within the striate cortex (Horton and Hocking, 1997) while the monocular crescent is at one end of the representation (receiving fibers from the contralateral eye). The blind spot representation was not noted in our studies and it is unclear why this is so. The size of the blind spot representation in primates averages 5 × 2.5 mm (Horton and Hocking, 1996) whereas our voxel resolution was 2.5 mm in-plane with a slice thickness of 5 mm (blind spot representation has not been extensively studied in humans). So it may be that higher resolution fMRI will be required to further investigate this. In any case the blind spot representation would serve to further enhance the asymmetries present in the human visual cortex discussed so far and may contribute to the findings in this study.

A further subject for discussion concerns the total volume of activation for each eye. Rombouts *et al.* (1996) interestingly found that monocular stimulation tended to activate greater areas in the visual cortex of controls when the dominant eye was stimulated. For our study ocular dominance tests for the two groups of controls were not routinely measured and so we are unable to verify these observations. Our results indicated that the total mean volumes of visual cortex activation were not significantly different between left and right eye stimulation. Interestingly if the fifth subject of the 20-s group is excluded from the calculation then a significant difference is found in the total area of activation between left and right eye stimulation for that group. Future studies will be required to explore the relationship between visual cortical activation and ocular dominance.

Some limitations of this study will now be discussed and suggestions for future studies to validate and re-

fine the findings will be made. A periodic block experimental paradigm was performed because it is robust at producing reliable activation maps and in terms of fMRI design is the most efficient. Potential sources of bias should have been accounted for. Each eye was chosen at random for each subject. In addition, because our experimental design was exactly the same for each eye and each subject, any habituation bias should theoretically have been accounted for. However, future studies could be performed using an interleaved stimulus strategy or an event related design which would obviate these theoretical biases. With regard to our results, it is possible, though unlikely, that vascular morphology may influence the interpretation of the activation maps. The monocular crescent might be smaller than the increased area of activation in the posterior visual cortex and the asymmetry may be exaggerated by vascular anatomy. However, we do not believe that an asymmetry of activation of vascular structures could completely account for our findings and a retinotopic study would be important to clarify the reason for the observed asymmetrical activation patterns. Another study of interest would be to investigate the activation pattern in response to central visual field stimulation. By restricting the stimulus to central field, activation would theoretically be induced at the occipital poles only. Any asymmetries found therefore would result presumably from asymmetries of the ocular dominance columns.

In summary, we have demonstrated using fMRI that an asymmetry exists in the spatial distribution and response power of visual cortex activation in normal volunteers during monocular photic stimulation. This finding correlates well with the results of anatomical and neurophysiological studies of the visual system in primates which favor input from the contralateral eye at several levels of the visual pathway including the retina, optic chiasm, lateral geniculate nucleus, and visual cortex. In spite of this, it is important to note that structural connectivity and functional connectivity are not synonymous and additional explanations for the functional asymmetry may come to light in the future. Whatever the explanation, the results of this study suggest that it is important to take into account asymmetric visual cortex activation when performing fMRI studies of the visual system using monocular stimulation in patients and controls.

ACKNOWLEDGMENTS

This work was supported by The MS Society, The Barnwood House Trust, and the Mrs. F. B. Laurence Charitable Trust. We also thank David MacManus and Andrew Lowe for their help with scanning the subjects.

REFERENCES

Belliveau, J. W., Kennedy, D. N., Jr., McKinstry, R. C., Buchbinder, B. R., Weisskoff, R. M., Cohen, M. S., Vevea, J. M., Brady, T. J., and Rosen, B. R. 1991. Functional mapping of the human visual cortex by magnetic resonance imaging. *Science* **254:** 716–719.

Brammer, M. J., Bullmore, E. T., Simmons, A., Williams, S. C., Grasby, P. M., Howard, R. J., Woodruff, P. W., and Rabe-Hesketh, S. 1997. Generic brain activation mapping in functional magnetic resonance imaging: A nonparametric approach. *Magn. Reson. Imag.* **15:** 763–770.

Bullmore, E., Brammer, M., Williams, S. C., Rabe-Hesketh, S., Janot, N., David, A., Mellers, J., Howard, R., and Sham, P. 1996. Statistical methods of estimation and inference for functional MR image analysis. *Magn. Reson. Med.* **35:** 261–277.

Bullmore, E. T., Brammer, M. J., Rabe-Hesketh, S., Curtis, V. A., Morris, R. G., Williams, S. C., Sharma, T., and McGuire, P. K. 1999. Methods for diagnosis and treatment of stimulus-correlated motion in generic brain activation studies using fMRI. *Hum. Brain Map.* **7:** 38–48.

Chacko, L. W. 1948. The laminar pattern of the lateral geniculate body in the primate. *J. Neurol. Neurosurg. Psychiatry* **11:** 211–224.

Connolly, M., and Van Essen, D. 1984. The representation of the visual field in parvicellular and magnocellular layers of the lateral geniculate nucleus in the macaque monkey. *J. Comp. Neurol.* **226:** 544–564.

Cox, R. W. 1995. Analysis and visualisation of 3D fMRI data. In *Proceedings of the 3rd Scientific Meeting, Society of Magnetic Resonance*, Vol. 2, p. 834.

Hedera, P., Lai, S., Haacke, E. M., Lerner, A. J., Hopkins, A. L., Lewin, J. S., and Friedland, R. P. 1994. Abnormal connectivity of the visual pathways in human albinos demonstrated by susceptibility-sensitized MRI. *Neurology* **44:** 1921–1926.

Horton, J. C., Dagi, L. R., McCrane, E. P., and de Monasterio, F. M. 1990. Arrangement of ocular dominance columns in human visual cortex. *Arch. Ophthalmol.* **108:** 1025–1031.

Horton, J. C., and Hocking, D. R. 1996. Intrinsic variability of ocular dominance column periodicity in normal macaque monkeys. *J. Neurosci.* **16:** 7228–7239.

Horton, J. C., and Hocking, D. R. 1997. Timing of the critical period for plasticity of ocular dominance columns in macaque striate cortex. *J. Neurosci.* **17:** 3684–3709.

Howard, R., Williams, S., Bullmore, E., Brammer, M., Mellers, J., Woodruff, P., and David, A. 1995. Cortical response to exogenous visual stimulation during visual hallucinations [letter]. *Lancet* **345:** 70.

Hubel, D. H., and Wiesel, T. N. 1968. Receptive fields and functional architecture of monkey striate cortex. *J. Physiol. (London)* **195:** 215–243.

Hubel, D. H., and Wiesel, T. N. 1969. Anatomical demonstration of columns in the monkey striate cortex. *Nature* **221:** 747–750.

Itaya, S. K., and van Hoesen, G. W. 1982. WGA-HRP as a transneuronal marker in the visual pathways of monkey and rat. *Brain Res.* **236:** 199–204.

Kupfer, C., Chumbley, L., and Downer, J. C. 1967. Quantitative histology of optic nerve, optic tract and lateral geniculate nucleus of man. *J. Anat.* **101:** 393–401.

Kwong, K. K., Belliveau, J. W., Chesler, D. A., Goldberg, I. E., Weisskoff, R. M., Poncelet, B. P., Kennedy, D. N., Hoppel, B. E., Cohen, M. S., Turner, R., Cheng, H-M., Brady, T. J., and Rosen, B. R. 1992. Dynamic magnetic resonance imaging of human brain activity during primary sensory stimulation. *Proc. Natl. Acad. Sci. USA* **89:** 5675–5679.

Le Gros Clark, W. E. 1941. The laminar organization and cell content of the lateral geniculate body in the monkey. *J. Anat.* **75:** 419–433.

LeVay, S., Connolly, M., Houde, J., and Van Essen, D. C. 1985. The complete pattern of ocular dominance stripes in the striate cortex and visual field of the macaque monkey. *J. Neurosci.* **5:** 486–501.

LeVay, S., Wiesel, T. N., and Hubel, D. H. 1980. The development of ocular dominance columns in normal and visually deprived monkeys. *J. Comp. Neurol.* **191:** 1–51.

Miki, A., Nakajima, T., Takagi, M., Shirakashi, M., and Abe, H. 1996. Detection of visual dysfunction in optic atrophy by functional magnetic resonance imaging during monocular visual stimulation. *Am. J. Ophthalmol.* **122:** 404–415.

Ogawa, S., Tank, D. W., Menon, R., Ellermann, J. M., Kim, S. G., Merkle, H., and Ugurbil, K. 1992. Intrinsic signal changes accompanying sensory stimulation: Functional brain mapping with magnetic resonance imaging. *Proc. Natl. Acad. Sci. USA* **89:** 5951–5955.

Perry, V. H., and Cowey, A. 1985. The ganglion cell and cone distributions in the monkey's retina: Implications for central magnification factors. *Vision Res.* **25:** 1795–1810.

Polyak, S. 1957. *The Vertebrate Visual System*. The University of Chicago Press, Chicago.

Rombouts, S. A., Barkhof, F., Sprenger, M., Valk, J., and Scheltens, P. 1996. The functional basis of ocular dominance: Functional MRI (fMRI) findings [published erratum appears in *Neurosci. Lett.*, 1997, Mar 14; **224**(2) :147]. *Neurosci. Lett.* **221:** 1–4.

Rombouts, S. A., Lazeron, R. H., Scheltens, P., Uitdehaag, B. M., Sprenger, M., Valk, J., and Barkhof, F. 1998. Visual activation patterns in patients with optic neuritis: An fMRI pilot study. *Neurology* **50:** 1896–1899.

Rosa, M. G., Gattass, R., and Fiorani Junior, M. 1988. Complete pattern of ocular dominance stripes in V1 of a New World monkey, *Cebus apella. Exp. Brain Res.* **72:** 645–648.

Sereno, M. I., Dale, A. M., Reppas, J. B., Kwong, K. K., Belliveau, J. W., Brady, T. J., Rosen, B. R., and Tootell, R. B. 1995. Borders of multiple visual areas in humans revealed by functional magnetic resonance imaging. *Science* **268:** 889–893.

Silveira, L. C., Perry, V. H., and Yamada, E. S. 1993. The retinal ganglion cell distribution and the representation of the visual field in area 17 of the owl monkey, *Aotus trivirgatus. Vis. Neurosci.* **10:** 887–897.

Stone, J. 1966. The naso-temporal division of the cat's retina. *J. Comp. Neurol.* **126:** 585–600.

Stone, J., and Hansen, S. M. 1966. The projection of the cat's retina on the lateral geniculate nucleus. *J. Comp. Neurol.* **126:** 601–624.

Stone, J., Leicester, J., and Sherman, S. M. 1973. The naso-temporal division of the monkey's retina. *J. Comp. Neurol.* **150:** 333–348.

Talairach, J., and Tournoux, P. 1988. *Co-planar Stereotaxic Atlas of the Human Brain.* Thieme, New York.

Thomas, C. G., and Menon, R. S. 1998. Amplitude response and stimulus presentation frequency response of human primary visual cortex using BOLD EPI at 4T. *Magn. Reson. Med.* **40:** 203–209.

Tootell, R. B., Switkes, E., Silverman, M. S., and Hamilton, S. L. 1988. Functional anatomy of macaque striate cortex. II. Retinotopic organization. *J. Neurosci.* **8:** 1531–1568.

Tootell, R. B., Hadjikhani, N. K., Vanduffel, W., Liu, A. K., Mendola, J. D., Sereno, M. I., and Dale, A. M. 1998. Functional analysis of primary visual cortex (V1) in humans. *Proc. Natl. Acad. Sci. USA* **95:** 811–817.

Tychsen, L., and Burkhalter, A. 1997. Nasotemporal asymmetries in V1: ocular dominance columns of infant, adult, and strabismic macaque monkeys. *J. Comp. Neurol.* **388:** 32–46.

Walsh, T. J. 1974. Temporal crescent or half-moon syndrome. *Ann. Ophthalmol.* **6:** 501–505.

Werring, D. J., Bullmore, E. T., Toosy, A. T., Miller, D. H., Barker, G. J., MacManus, D. G., Brammer, M. J., Giampietro, V. P., Brusa, A., Brex, P. A., Moseley, I. F., Plant, G. T., McDonald, W. I., and Thompson, A. J. 2000. Recovery from optic neuritis is associated with a change in the distribution of cerebral response to visual stimulation: A functional magnetic resonance imaging study. *J. Neurol. Neurosurg. Psychiatry* **68:** 441–449.